Biochimica et Biophysica Acta 1798 (2010) 194–201

Contents lists available at ScienceDirect

Biochimica et Biophysica Acta

journal homepage: www.elsevier.com/locate/bbamem

Nuclear magnetic resonance evidence for retention of a lamellar membrane phase with curvature in the presence of large quantities of the HIV fusion peptide

Charles M. Gabrys, Rong Yang, Christopher M. Wasniewski, Jun Yang, Christian G. Canlas, Wei Qiang, Yan Sun, David P. Weliky *

Department of Chemistry, Michigan State University, East Lansing, MI 48824, USA

ARTICLE INFO

Article history:
Received 17 April 2009
Received in revised form 21 June 2009
Accepted 8 July 2009
Available online 17 July 2009

Keywords:
HIV
Fusion
Peptide
NMR
Curvature
Membrane

ABSTRACT

The HIV fusion peptide (HFP) is a biologically relevant model system to understand virus/host cell fusion. ^{2}H and ^{31}P NMR spectroscopies were applied to probe the structure and motion of membranes with bound HFP and with a lipid headgroup and cholesterol composition comparable to that of membranes of host cells of HIV. The lamellar phase was retained for a variety of highly fusogenic HFP constructs as well as a non-fusogenic HFP construct and for the influenza virus fusion peptide. The lamellar phase is therefore a reasonable structure for modeling the location of HFP in lipid/cholesterol dispersions. Relative to no HFP, membrane dispersions with HFP had faster ^{31}P transverse relaxation and faster transverse relaxation of acyl chain ^{2}H nuclei closest to the lipid headgroups. Relative to no HFP, mechanically aligned membrane samples with HFP had broader ^{31}P signals with a larger fraction of unoriented membrane. The relaxation and aligned sample data are consistent with bilayer curvature induced by the HFP which may be related to its fusion catalytic function. In some contrast to the subtle effects of HFP on a host-cell-like membrane composition, an isotropic phase was observed in dispersions rich in phosphatidylethanolamine lipids and with bound HFP.

1. Introduction

Membrane fusion plays an essential role in enveloped virus entry into target host cells [1]. For the human immunodeficiency virus (HIV), fusion occurs directly between the viral and target cell membranes with subsequent formation of a single membrane enclosing the viral and host cell contents. Membrane fusion is carefully controlled on a spatial and temporal basis so as to keep the host cell intact for viral replication. Fusion is aided by interaction between the target cell membrane and the ~20-residue N-terminal "fusion peptide" (HFP) domain of the gp41 viral envelope protein [1,2].

Peptides with the HFP sequence have been shown to induce fusion between liposomes and between erythrocytes, and numerous mutational studies have shown strong correlations between fusion peptide-induced liposome fusion and virus/host cell fusion [2]. These data support the study of the HFP/membrane interaction. The structure of the HFP has been studied by a variety of methods and there is an experimentally-based high-resolution secondary and tertiary structure model of the HFP in membranes whose lipid headgroup and cholesterol composition are comparable to that of host cells of the virus [3].

Studies have also been carried out on the location of the HFP in the membrane and on the effect of the HFP on membrane structure and motion. The Ala-1 to Gly-3 and Ala-14 to Gly-16 regions of the HFP are in close contact with lipid headgroups while the Ala-6 to Leu-12 region appears to be more deeply inserted into the membrane interior [4,5]. There are also reports that the HFP or the related simian immunodeficiency virus fusion peptide induces a non-lamellar phase for lipid compositions rich in phosphatidylethanolamine (PE) [6–8]. This result has been correlated with the observation that HFP and other viral fusion peptides promote the formation of the inverted hexagonal phase, which has negative curvature [9,10]. These data may relate to the fusion mechanisms through the "stalk" intermediates in which the contacting monolayers have negative curvature [11,12]. The fusion peptide may promote formation of stalk intermediates by inducing equilibrium negative curvature [13].

Development of high-resolution structural models for the HFP/membrane interaction will require better understanding of the dependence of the lipid and cholesterol phase on HFP construct as well as lipid and cholesterol composition. In this paper, ^{2}H and ^{31}P nuclear magnetic resonance (NMR) spectroscopies were applied to study the structure and motion of membranes with bound HFP. ^{2}H NMR spectra are dominated by the quadrupole interaction with the local electric field gradient. In unaligned samples, each ^{2}H produces a powder pattern with two distinct peaks whose frequency separation provides information on segmental motion [14,15]. Measurement of the longitudinal (T_1) and transverse (T_2) spin relaxation times provides information on the motions of phospholipid molecules [14,16]. The longitudinal relaxation rate is sensitive to fast motions having correlation times $\tau_1 \leq \omega_0^{-1}$ (where ω_0 is the nuclear Larmor

* Corresponding author. Tel.: +1 517 355 9715; fax: +1 517 353 1793.
E-mail address: weliky@chemistry.msu.edu (D.P. Weliky).

0005-2736/$ – see front matter © 2009 Elsevier B.V. All rights reserved.
doi:10.1016/j.bbamem.2009.07.007

frequency), including transitions between different molecular conformations and rotations of the molecules around the bilayer normal whereas the transverse relaxation rate is also sensitive to slow motions with correlation times $\tau_2 \gg \omega_0^{-1}$ [14,17]. The slow motions that contribute to transverse relaxation can be interpreted to be from molecular diffusion along curved membrane surfaces [17].

2. Materials and methods

2.1. Materials

Rink amide resin was purchased from Advanced Chemtech (Louisville, KY), and 9-fluorenylmethoxycarbonyl (FMOC)-amino acids were obtained from Peptides International (Louisville, KY). Labeled amino acids were purchased from Icon Services Inc. (Summit, NJ) or from Cambridge Isotopes (Andover, MA) and the FMOC group was added using literature methods [18,19]. 1,2-Dimyristoyl(d_{54})-*sn*-glycero-3-phosphocholine (DMPCdac), 1-palmitoyl-2-oleoyl-*sn*-glycero-3-phosphocholine (POPC), 1-palmitoyl-2-oleoyl-*sn*-glycero-3-phosphoethanolamine (POPE), 1-palmitoyl-2-oleoyl-*sn*-glycero-3-[phospho-L-serine] (POPS), phosphatidylinositol (PI), sphingomyelin, *N*-(7-nitro-2,1,3-benzoxadiazol-4-yl)-phosphatidylethanolamine (*N*-NBD-PE), *N*-(lissamine Rhodamine B sulfonyl)-phosphatidylethanolamine (*N*-Rh-PE), 1,2-dioleoyl-*sn*-glycero-3-phosphocholine (DOPC), 1,2-dioleoyl-*sn*-glycero-3-phosphoethanoloamine (DOPE), 1,2-*O*-ditetradecyl-*sn*-glycero-3-phosphocholine (DTPC), 1,2-*O*-ditetradecyl-*sn*-glycero-3-[phospho-*rac*-(1-glycerol)] (DTPG), 1-palmitoyl-2-(5-fluoropalmitoyl)-*sn*-glycero-3-phosphocholine (DPPC-F(C5)), and cholesterol were purchased from Avanti Polar Lipids (Alabaster, AL). The BCA protein assay was obtained from Pierce (Rockford, IL). *N*-2-hydroxyethylpiperazine-*N*′-2-ethanesulfonic acid (HEPES) and Triton X-100 were obtained from Sigma (St. Louis, MO).

2.2. Peptides

HFP contained the 23 N-terminal residues of HIV gp41 (AVGIGALFLGFLGAAGSTMGARS) and was synthesized as a C-terminal amide using a peptide synthesizer (ABI 431A, Foster City, CA) equipped for FMOC chemistry. HFP_K3 with sequence AVGIGALFLGFLGAAGSTMGARSKKK contained three non-native C-terminal lysines which improved aqueous solubility. HFP_K5 had sequence AVGIGALFLGFLGAAGSTMGARSWKKKKKA and HFPmut_K5 had sequence AEGIGALFLGFLGAAGSTMGARSWKKKKKA with the V2E mutation and is a non-fusogenic mutant in HIV and as a peptide [20,21]. HFPtr_K5 contained three HFP_K5 strands that were chemically cross-linked at their C-termini to form a HFP trimer which is the putative oligomeric state of gp41 [5]. The influenza virus fusion peptide (IFP_K4) had sequence GLFGAIAGFIENGWEGMIDGGGKKKKG where the seven C-terminal residues are a solubility tag [22]. Melittin with sequence GIGAVLKVLTTGLPALISWIKRKRQQ is the major component of bee venom and served as a model lytic peptide [23,24].

2.3. Membrane preparation

Samples were usually prepared with a lipid/cholesterol mixture that reflects the approximate lipid and cholesterol content of the host cells of HIV [25,26]. One mixture, denoted "LM3," had POPC, POPE, POPS, sphingomyelin, PI, and cholesterol in a 10:5:2:2:1:10 mol ratio. Another mixture, denoted "LM3-DMPCdac" had DMPCdac, POPE, POPS, sphingomyelin, PI, and cholesterol in a 10:5:2:2:1:10 mol ratio. The DMPCdac was perdeuterated along the acyl sidechains. Some of the samples were prepared with DTPC:DTPG:DPPC-F(C5):cholesterol in a 8:2:1:5 mol ratio. This composition also reflected the cholesterol content and large fraction of lipids with choline headgroups in membranes of host cells of HIV. The DTPG reflected negatively charged lipids in these membranes and the DPPC-F(C5) provided ^{19}F which is a useful lipid probe nucleus for future NMR experiments. The DTPC and DTPG lipids contained ether- rather than ester-linkages which greatly reduce the lipid natural abundance contribution to the ^{13}CO signal. This reduction is very useful in measurements of peptide ^{13}CO-lipid ^{31}P and peptide ^{13}CO-lipid ^{19}F distances which provide experimental constraints on peptide location in the membrane [4,5]. It is noted that PG is not the anionic lipid found in mammalian cell membranes. Lipid and cholesterol powders were dissolved together in chloroform. The chloroform was removed under a stream of nitrogen gas followed by overnight vacuum pumping. Lipid dispersions were formed by addition of water or buffer followed by homogenization with freeze–thaw cycles. In some cases, large unilamellar vesicles (LUVs) of 100 nm diameter were prepared by extrusion.

2.4. Lipid mixing assay for membrane fusion

Two types of LM3 LUVs were prepared [27]. One set contained 2 mol% of the fluorescent lipid *N*-NBD-PE and 2 mol% of the quenching lipid *N*-Rh-PE while the other set only contained unlabeled lipids. Fluorescently labeled and unlabeled vesicles were mixed in a 1:9 ratio. Following addition of peptide, lipid mixing between labeled and unlabeled vesicles caused dilution of the labeled lipids with a resulting increase of fluorescence. Fluorescence was recorded using 4 nm bandwidth on a fluorimeter operating at excitation and emission wavelengths of 465 nm and 530 nm, respectively (Instruments S.A. Fluoromax-2, Edison, NJ). Measurements were carried out with continuous stirring at 37 °C with 2 ml of 150 μM LUVs in 5 mM HEPES at pH 7.0. An aliquot of aqueous 0.5 mM peptide solution was added to achieve the desired peptide:lipid mol ratio, and the change in fluorescence of the sample was monitored following this addition. The initial fluorescence intensity F_0 referenced zero lipid mixing and the maximum fluorescence intensity F_{max} was obtained following addition of 20 μl of 10% Triton X-100. Percent lipid mixing at time t was given by $[(F_t - F_0)/(F_{max} - F_0)] \times 100$.

2.5. Membrane dispersion sample preparation

Peptide solutions were mixed with aqueous dispersions of lipid and cholesterol usually in 5 mM HEPES buffer at pH 7.0. The samples lacked physiologically relevant dissolved salt because salt causes aggregation of the HFP [28]. In some cases, particularly the magic angle spinning (MAS) samples, membrane LUVs were initially prepared and after peptide binding, the LUVs with bound peptide were centrifuged to form a more concentrated sample. Electron micrographs have shown that after HFP binding, the final membrane morphology is large aggregates of fused vesicles [29]. ^{2}H-depleted water was used for samples prepared for ^{2}H NMR spectroscopy.

2.6. Oriented sample preparation

Microscope cover slips were cut to fit inside a glass tube which was either cylindrical with a 5 mm diameter or cubic with a 10 mm × 10 mm cross-section. A 50 μl aliquot of hydrated membrane dispersion or dispersion plus fusion peptide was placed on each slide. Each aliquot contained 1.0–1.5 mg of lipid. Over the course of one to two days, bulk water was allowed to evaporate. The plates were then stacked inside the glass tube, and the tube was placed inside a bottle containing saturated $(NH_4)_3PO_4$ solution. The sealed bottle was placed in an incubator at 35–40 °C for a few days so that the plates were in vapor contact with a 90% humidity environment. The tube was then removed from the bottle, and a specially machined Kel-F plug was inserted into its open end and then sealed with epoxy. In these sealed samples, the lipids remain hydrated and oriented over the course of at least one month.

2.7. REDOR NMR

Rotational-echo double-resonance (REDOR) spectroscopy was performed on a 9.4 T spectrometer (Varian Infinity Plus, Palo Alto, CA) using a triple resonance MAS probe equipped with a 6 mm diameter rotor [30]. The NMR detection channel was tuned to ^{13}C, the decoupling channel was tuned to ^{1}H, and the third channel was tuned to ^{15}N. Experiments were carried out using a MAS frequency of 8000 ± 2 Hz. Cross-polarization at 50 kHz for 1.2 ms was followed by a 1 ms REDOR dephasing period and then direct ^{13}C detection. A single 50 kHz ^{13}C refocusing π pulse at 155 ppm was placed at the center of the dephasing time, and ^{1}H TPPM decoupling at 65 kHz was applied during both dephasing and detection [31]. For the S_1 acquisition, the dephasing time contained a 40 kHz ^{15}N π pulse at the middle and end of each rotor period, while the S_0 acquisition did not contain these pulses. XY-8 phase cycling was used for the ^{15}N pulses and the ^{15}N frequency was near the isotropic peptide amide resonance [32,33]. The recycle delay was 1 s. Chemical shifts were referenced to the methylene carbon resonance of adamantane at 40.5 ppm [34].

2.8. Static NMR

Experiments were done on a 9.4 T spectrometer (Varian VXR or Varian Infinity Plus, Palo Alto, CA) using either a Varian single or triple resonance probe or a home-built double resonance probe. The NMR detection channel was tuned to ^{2}H or ^{31}P and the decoupling channel was tuned to ^{1}H. RF fields of about 40 kHz, 50 kHz, and 40 kHz were used for ^{2}H, ^{31}P, and ^{1}H, respectively.

For ^{2}H, the quadrupolar echo sequence $(\pi/2)-\tau_1-(\pi/2)-\tau_2-$acquire was used to minimize effects from probe ring-down. The phase of the first $\pi/2$ pulse was x and the phase of the second $\pi/2$ pulse alternated between y and $-y$. The recycle delay was 1 s. To determine the ^{2}H T_2, the decay of the acquired signal was measured as a function of synchronous incrementation of τ_1 and τ_2. To determine the ^{2}H T_1, a $(\pi)_x-d_1$ inversion-recovery module was inserted before the echo sequence, and the variation of the acquired signal was measured as a function of d_1.

For ^{31}P experiments, Bloch decay spectra with ^{1}H decoupling were taken using a recycle delay of 3 or 4 s and CYCLOPS phase cycling [35]. The ^{31}P chemical shifts were referenced to either phosphoric acid at 0.0 ppm, triphenylphosphite at 130.0 ppm, or triphenylphosphate at −17.6 ppm. The ^{31}P T_2 measurements were done using a chemical shift echo sequence $\pi/2-\tau-\pi-\tau-$acquire and the total echo times ranged from 480–1560 μs.

3. Results

3.1. Representative fusogenicity and MAS NMR spectra

HFP, HFP_K3, and HFPtr_K5 all induce significant vesicle fusion and representative lipid mixing data for HFP_K3 are displayed in Fig. 1a. These results are comparable to those obtained for HFP and indicate that addition of the three C-terminal lysines does not affect the fusogenicity of the peptide. HFPtr_K5 induces even more rapid vesicle fusion [5,36]. In membranes with physiologically relevant cholesterol content, the 16 N-terminal residues of HFP, HFP_K3, HFPmut_K5, and HFPtr_K5 adopt predominant β strand conformation, as primarily evidenced by ^{13}C chemical shifts [3,5,28,36]. Fig. 1b, c displays representative ^{13}C REDOR difference spectra of HFP and HFP_K3 associated with LM3 membranes. Because of the specific isotopic labeling and the REDOR approach, natural abundance signals are filtered out and only the signal from the labeled Phe-8 carbonyl is detected in each spectrum [37,38]. For both samples, the spectra are very similar and consist of a single line centered at 173 ppm which correlated with β strand rather than with helical or coil conformation and is similar to the spectrum observed for LM3-associated HFPtr_K5 [36,39].

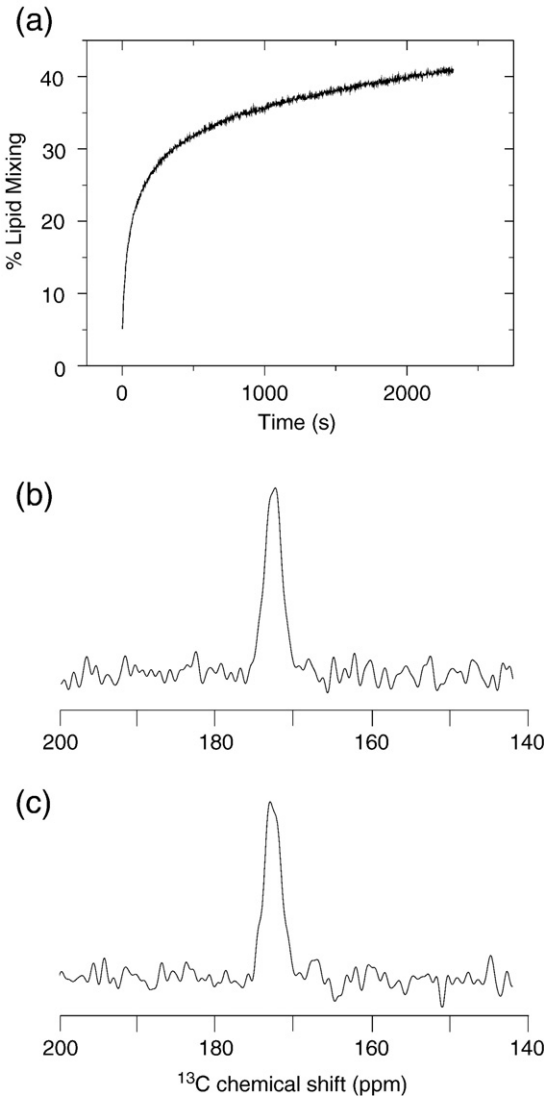

Fig. 1. (a) HFP_K3-induced lipid mixing of LM3 LUVs at 37 °C with HFP_K3, total lipid, and cholesterol concentrations of 1.5, 150, and 75 μM, respectively. (b, c) REDOR-filtered magic angle spinning ^{13}C NMR spectra of LM3-associated HFP and HFP_K3, respectively. The peptides were ^{13}CO labeled at Phe-8 and ^{15}N labeled at Leu-9 and the S_0-S_1 spectra were dominated by the Phe-8 ^{13}CO signal whose peak chemical shift was consistent with β strand conformation. The samples contained 0.4 μmol peptide, 40 μmol total lipid, and 20 μmol cholesterol and were cooled with nitrogen gas at −50 °C. Each spectrum was the sum of ~10000 acquisitions and was processed with 50 Hz line broadening.

3.2. Static NMR spectra

Fig. 2 displays representative NMR spectra of static samples containing lipid/cholesterol dispersions where panels a–e are ^{2}H spectra and panels f–i are ^{31}P spectra. The a–h samples were made with LM3 and the i sample was made with DOPC:DOPE:cholesterol. Several of the samples were made a second time and the spectra were reproducible, in particular sample i whose lineshape differs significantly from the other ^{31}P NMR spectra. Samples were also prepared with and without the LUV step and by simple mixing of peptide, lipids, and cholesterol and yielded similar spectra independent of preparation method. In addition, the ^{31}P NMR spectra of the a–c samples are similar to those of the f–h spectra, indicating that the ^{31}P lineshape is approximately independent of DMPC or POPC

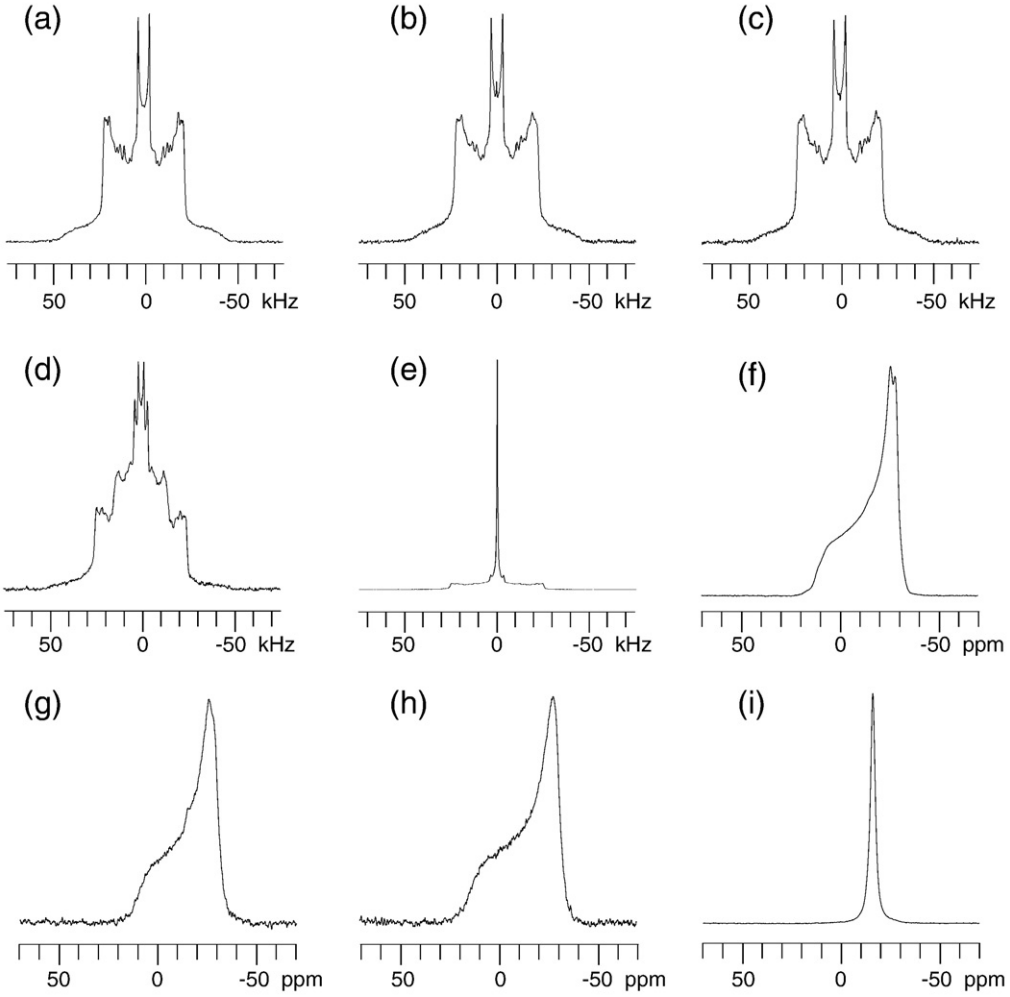

Fig. 2. NMR spectra of lipid/cholesterol dispersions with peptides. ^{2}H spectra are displayed in panels a–e and the samples contained LM3-DMPCdac dispersions with peptide and peptide:total lipid (excluding cholesterol) mol ratios: (a) no peptide; (b) HFP, 0.03; (c) HFP, 0.10; (d) melittin, 0.03; and (e) melittin, 0.10. ^{31}P spectra are displayed in panels f–h and the samples contained LM3 dispersions with peptide and peptide:lipid mol ratios: (f) no peptide; (g) HFP, 0.02; and (h) HFP_K3, 0.02. A similar ^{31}P spectrum is displayed in panel i and contained HFP:total lipid = 0.02 with the dispersion composed of DOPC:DOPE:cholesterol in a 1:1:1 mol ratio. A typical sample contained ~30 μmol total lipid and ~15 μmol cholesterol. The ^{2}H and ^{31}P spectra were obtained at 35 °C, were respectively processed with 150 or 50 Hz line broadening, and were respectively the sums of 4000 to 6000 scans or 5000 to 20000 scans.

lipid, the mol ratio of HFP to lipid in the 0 to 0.10 range, and the presence of the K3 solubility tag.

Each ^{2}H spectrum in panels a–e is a superposition of individual Pake powder patterns of the ^{2}H nuclei along the DMPC acyl chains. Each methylene position experiences a different amount of motion and thus has a different quadrupolar splitting. The motion increases and the quadrupolar splitting decreases from the headgroup to the tail. As displayed in panels a–c, there were minor changes in the ^{2}H NMR spectra with addition of HFP. Relative to the pure LM3-DMPCdac sample, binding of HFP appears to cause some small increases in quadrupolar splittings in the range of 1–3% and 2–5% for HFP:lipid = 0.03 and 0.1, respectively. This is consistent with less chain motion in the presence of HFP. In addition, the peaks of the individual Pake patterns are broader in the presence of HFP, consistent with a more heterogeneous distribution of lipid motion. Both of these small changes are consistent with some interference with lipid motion by the incorporation of HFP into the membrane. Overall, the ^{2}H spectra support retention of the membrane bilayer phase for LM3 even with large quantities of HFP.

In some contrast, panel e with melittin:lipid = 0.10 shows a narrow, isotropic ^{2}H feature, which has ~200 Hz FWHM linewidth and which is shifted about 300 Hz upfield of the signal of a $^{2}H_2O$ reference sample. The narrow feature is likely associated with formation of an isotropic, non-lamellar lipid/cholesterol phase. Overall, panels a–e indicate that the lytic peptide melittin affects the LM3 dispersion very differently than does HFP.

Consistent with the ^{2}H spectra, the ^{31}P NMR spectra displayed in panels f–h show relatively minor effects from the addition of HFP. The spectrum of the pure LM3 sample in panel f is consistent with a predominant lamellar phase [40]. In addition, there is a clear splitting at the low ppm edge with peaks at −25.7 and −28.2 ppm and less apparent splitting at the high ppm edge with shoulders at 7 and 12 ppm. Assuming that the isotropic ^{31}P chemical shift is approximately the same for all lipids, the most reasonable explanation for these splittings is that there is a superposition of two powder patterns with chemical shift anisotropies (CSAs) of 33 and 40 ppm. The spectra g and h of the samples containing HFP or HFP_K3 are also consistent with a predominant lamellar phase. In spectrum g, the upfield splitting is apparent as a −28.5 ppm shoulder on the −26 ppm peak. The splitting is less clear than in the pure LM3 sample, probably because of broadening of the individual powder patterns. This effect is similar to the observed broadening of the ^{2}H features in the presence of HFP and is consistent with a more heterogeneous distribution of lipid headgroup motions. When spectrum f (sample without HFP) is processed with 300 Hz line broadening, its lineshape is similar to

that of spectrum g with HFP. One minor difference is the small feature at −15 ppm in spectrum g, which may indicate some small fraction of isotropic lipid/cholesterol phase [40–42]. This feature is less apparent in spectrum f and is not apparent in spectrum h which was prepared with HFP_K3.

The ^{31}P spectrum in panel i for the DOPC:DOPE:cholesterol mixture with HFP correlates with a predominant isotropic rather than lamellar phase and is consistent with the work of other investigators and is different than spectra g–h observed for LM3 with HFP or HFP_K3 [8]. In addition, at room temperature the spectrum for this sample broadened significantly, suggesting that there is a phase transition between 20 °C and 35 °C. In the absence of HFP, the ^{31}P spectrum for DOPC:DOPE:cholesterol appeared to be a superposition of lamellar and isotropic phase spectra. Thus, for DOPC:DOPE:cholesterol, HFP appears to induce significantly greater isotropic phase while our ^{2}H and ^{31}P spectra do not support this conclusion for LM3. The greatest compositional difference between LM3 and the DOPC:DOPE:cholesterol mixture is the lipid mol fraction of PE lipid, 0.25 for the former and 0.50 for the latter composition. PE lipids are widely used for their propensity to transit between lamellar and non-lamellar phases [43].

Fig. 3 displays additional ^{31}P NMR spectra of samples that contained lipid/cholesterol dispersions with composition DTPC:DTPG:DPPC-F(C5):cholesterol in a 8:2:1:5 mol ratio. Fig. 3 spectra are consistent with retention of the lamellar phase in samples containing fusogenic HFP_K5, highly fusogenic HFPtr_K5, non-fusogenic HFPmut_K5, and IFP_K4 at fusogenic pH 5.0 or less fusogenic pH 7.4. The somewhat different lineshapes of Fig. 2f–h and Fig. 3 spectra are likely due to differences in lipid compositions. In Fig. 2f–h, the samples contained LM3 which had five different lipid types with individual ^{31}P lineshapes that are likely somewhat different from one another. In Fig. 3, the composition was simpler with three different lipid types and ~75% of the total lipid was DTPC.

3.3. ^{2}H and ^{31}P relaxation times

^{2}H longitudinal and transverse times were determined for dispersions containing LM3-DMPCdac dispersions and HFP. The data were intensities of "outer" and "inner" spectral features as defined in Fig. 4a where the outer feature is mostly due to ^{2}H close to the headgroups and the inner feature is mostly due to ^{2}H in the terminal methyl group. The outer feature intensity was measured relative to the spectral baseline while the inner feature intensity was measured relative to an approximate baseline atop the non-methyl ^{2}H transitions.

T_1 values were determined by fitting the intensities of the inversion-recovery spectra as a function of the delay d_1:

$$I(d_1) = I_i + \left\{\Delta I \times \left(1 - e^{-d_1/T_1}\right)\right\} \quad (1)$$

where $I(d_1)$ is the measured echo intensity and fitting parameters are the initial echo intensity I_i, the difference ΔI between the equilibrium and initial echo intensities, and T_1.

Fig. 4b displays the outer feature inversion-recovery data for LM3-DMPCdac dispersions with HFP:lipid = 0 or 0.10. The best-fit relaxation times for these and other data sets are presented in Table 1. Within our fitting uncertainties, there is no difference among the outer feature T_1 values or among the inner feature T_1 values at different HFP concentrations. The relative uncertainties of the inner feature T_1 values are greater than those of the outer feature values, in part because of the uncertainty in determining the inner feature baseline.

^{2}H T_2 values were determined from measurements of the echo intensity as a function of the total echo time, 2τ, where τ is the time from the end of the second $\pi/2$ pulse to the echo formation. The data were fitted with:

$$\ln[I(2\tau)] = \ln[I(0)] - 2\tau/T_2 \quad (2)$$

where $I(2\tau)$ is the measured echo intensity and $I(0)$ and T_2 are fitting parameters. Fig. 4c displays plots of the outer feature data for the three different samples, and the best-fit T_2 values are listed in Table 1. There appears to be a 10–15% reduction in the outer feature T_2 with addition of HFP and this reduction was also observed for HFP_K3. The inner feature intensity data are the same within the listed uncertainties for the three samples.

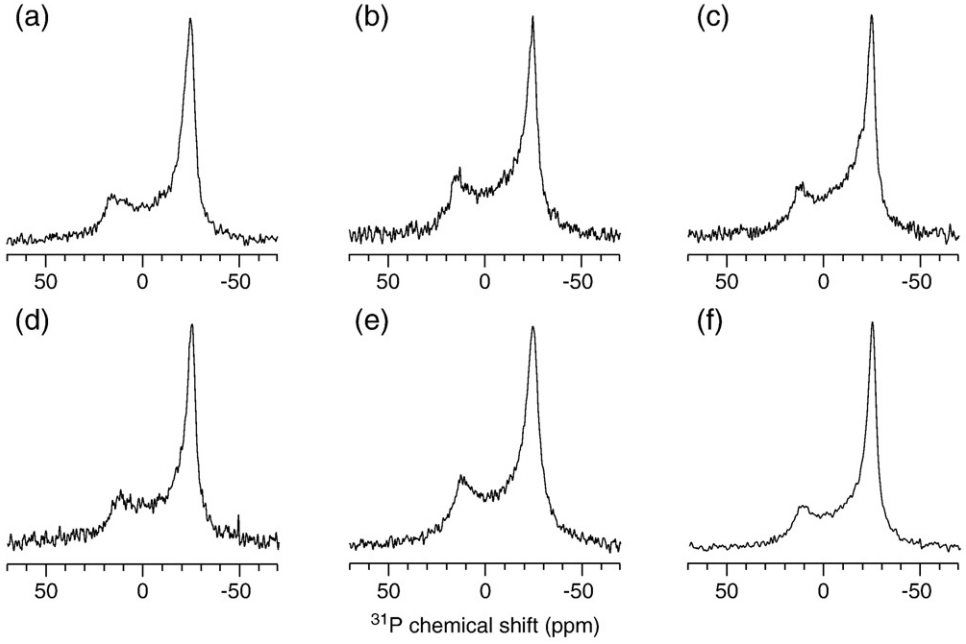

Fig. 3. ^{31}P NMR spectra at 35 °C of dispersion samples composed of DTPC:DTPG:DPPC-F(C5):cholesterol (8:2:1:5 mol ratio) with peptide and peptide:lipid mol ratios: (a) no peptide; (b) HFP_K5, 0.04; (c) HFPmut_K5, 0.04; (d) HFPtr_K5, 0.013; (e) IFP_K4 at pH 5.0, 0.04; (f) IFP_K4 at pH 7.4, 0.04. Each spectrum was processed with 100–150 Hz line broadening and was the sum of 300 to 1000 scans.

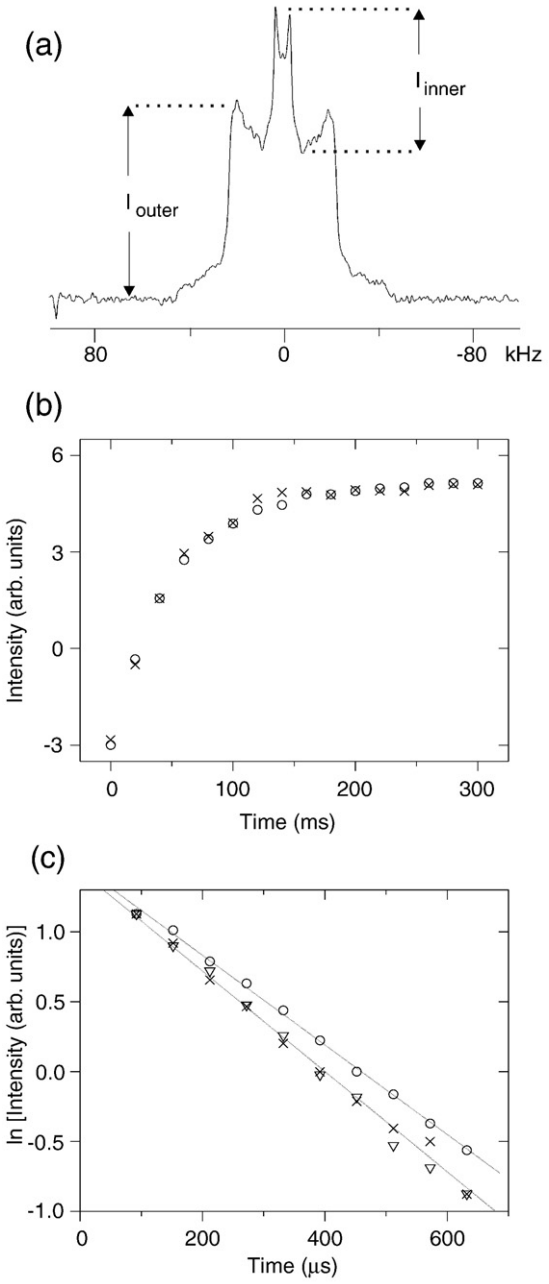

Fig. 4. (a) ^{2}H NMR spectrum of a LM3-DMPCdac dispersion sample showing "inner" and "outer" peak intensities which respectively correspond to terminal C^2H_3 and to C^2H_2 closest to the lipid headgroups. (b) Outer peak intensities vs delay time d_1 in the inversion-recovery pulse sequence. (c) ln(outer peak intensity) vs echo time 2τ in the quadrupolar echo sequence. The circles, triangles, and crosses respectively correspond to HFP:lipid = 0, 0.03, and 0.10. Panel c also displays best-fit lines for HFP:lipid = 0 and 0.10.

^{31}P T_2 values were measured on LM3 and LM3-DMPCdac dispersions with HFP_K3:lipid = 0 or 0.03. The T_2 values were determined from measurements of the echo intensities and fitting with Eq. (2) as described for ^{2}H above, and the best-fit T_2 values are displayed in Table 2. T_2 is 30–40% lower for the samples that contain HFP_K3.

3.4. NMR spectra of aligned samples

Fig. 5 displays representative ^{31}P NMR spectra of oriented glass plate samples containing LM3 and HFP_K3:lipid of (a, b) 0 or (c, d) 0.02. In (a, c) the glass plate normal and magnetic field were parallel, and in (b, d) the normal and field were perpendicular. In the absence of HFP_K3, there is a narrow, dominant ^{31}P feature with peak chemical shift 10.4 ppm for the parallel orientation and −27.7 ppm for the perpendicular orientation. The observed chemical shifts indicate that the lipids are in the lamellar phase and that the lamellae are oriented with their normal approximately parallel to the glass plate normal. The CSA is ~38 ppm and lies between the 33 and 40 ppm CSAs of the powder patterns observed in the dispersion sample in Fig. 2f. In another aligned sample, the perpendicular spectrum showed two peaks at −28.1 and −25.9 that likely correspond to the perpendicular edges of the powder patterns. In Fig. 5a,b, there are additional small features at 22, 18, and 0 ppm in the (a) parallel orientation and −33, −31, and −22 ppm in the (b) perpendicular orientation. These likely represent minor populations of oriented lipids whose CSAs are slightly different from the CSA of the lipids in the main peak. Assuming that all of the lipids have approximately the same isotropic ^{31}P chemical shift, −15 ppm, and considering the relative intensities in the parallel and perpendicular spectra, the most reasonable interpretation of the minor peaks is that they arise from three minor lipid populations with parallel and perpendicular shifts of 22 and −33 ppm (first population), 18 and −31 ppm (second population), and 0 and −22 ppm (third population). In addition, the parallel spectrum (a) also has a small, broad component with an upfield edge near −28 ppm. This feature is likely part of the powder pattern of unoriented lipid corresponding to the LM3 dispersion in Fig. 2f. Integration of the oriented and unoriented features is consistent with a ~5% population of unoriented lipid.

In the presence of HFP_K3, Fig. 5c, d, the ^{31}P spectra are significantly broader, and the unoriented component represents ~20% of the total signal. The dominant oriented peaks fall at 10.6 and −28.4 ppm in the parallel and perpendicular orientations, respectively, which are close to the values observed in the a,b spectra of samples without HFP_K3.

Table 1
Best-fit ^{2}H T_1 and T_2 values of DMPCdac sidechains in LM3-DMPCdac dispersions at 35 °C.

HFP:lipid	Peak feature	T_1 (ms)	T_2 (μs)
0	Outer	53 (1)	327 (10)
	Inner	340 (10)	794 (53)
0.03	Outer	50 (2)	268 (5)
	Inner	320 (60)	794 (84)
0.10	Outer	51 (2)	294 (10)
	Inner	310 (60)	709 (50)

Uncertainties are in parentheses.

4. Discussion

The interaction of the HFP with the host cell membrane is critical for fusion between the membranes of HIV and its host cell. There have been significant NMR studies delineating the structure of HFP in membranes whose "LM3" composition reflects the lipid headgroup and cholesterol composition of membranes of host cells of HIV [3,28]. There have also been NMR studies showing that the HFP induces formation of non-lamellar isotropic phases in lipid mixtures which have large fractions of PE [8]. Finally, there have been NMR measurements of distances between ^{13}CO nuclei in HFP and ^{31}P in phosphatidylcholine (PC)-rich membranes which indicate proximity

Table 2
Best-fit ^{31}P T_2 values in dispersions at 35 °C.

HFP_K3:lipid	Dispersion type	T_2 (μs)
0	LM3	2019 (98)
0	LM3-DMPCdac	2054 (72)
0.03	LM3	1171 (104)
0.03	LM3-DMPCdac	1459 (143)

Uncertainties are in parentheses.

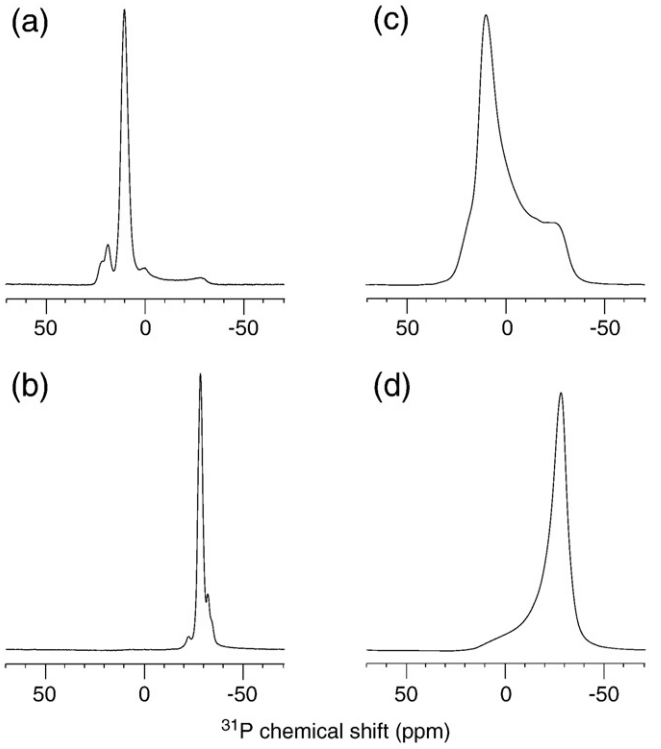

Fig. 5. ^{31}P NMR spectra of aligned samples containing LM3 with the glass plate normal either (a, c) parallel or (b, d) perpendicular to the magnetic field. The a, b sample did not contain peptide and the c, d sample contained HFP_K3 with HFP_K3:lipid mol ratio = 0.02. Spectra were obtained at 35 °C, processed with 25 Hz line broadening, and represented the sums of 10000 scans.

of the Ala-1 to Gly-3 and Ala-14 to Gly-16 regions to the lipid headgroups and insertion of the Ala-6 to Leu-12 region into the membrane interior [4,5]. In order to understand fusion as well as to properly interpret the HFP structure and membrane location measurements, it is important to understand the lipid/cholesterol phase with bound HFP as well as the dependence of this phase on lipid and cholesterol composition. One overall result from analysis of the ^{2}H and ^{31}P static NMR spectra is that at 35 °C, the lamellar phase is retained in PC-rich membranes even at HFP:lipid = 0.10 whereas a large fraction of isotropic phase is detected in PE-rich membranes. The former result holds true for a variety of HFP constructs including a non-fusogenic mutant as well as a highly active cross-linked trimer and also for the influenza virus fusion peptide. Membranes of host cells of HIV are PC-rich so it appears that HFP acts as a catalyst for membrane fusion but does not change the equilibrium lamellar phase. This is a biologically reasonable result because an intact host cell membrane is important for viability and consequent viral replication. This result also correlates with membrane stabilization by the final folded state of gp41 [44]. To date, studies of the location of HFP in lipid/cholesterol dispersions have been done with host-cell-like PC-rich lipid compositions and based on the data of the present study, it appears reasonable to use lamellar structure for the lipid/cholesterol phase in these models. The lytic peptide melittin disrupts PC-rich membranes which highlights the difference in membrane interaction of a peptide toxin and a peptide fusogen.

HFP does have some subtle effects on PC-rich membranes as evidenced by: (1) increases in the transverse relaxation rates of ^{31}P in the lipid headgroups and ^{2}H in acyl chain positions that are closest to the lipid headgroups; and (2) broadening of ^{31}P signals and an increase in the unoriented component in mechanically aligned membranes. These observations are consistent with measurements on other fusogenic peptides and with broad ^{15}N signals of HFP in mechanically aligned samples [22,45–47]. One interpretation of the changes in the NMR spectra and transverse relaxation rates is HFP-induced curvature in membranes. This curvature would result in a greater distribution of lipid molecule orientations in mechanically aligned samples and therefore a broader distribution of ^{31}P chemical shifts. Relative to a planar membrane, lipid molecule translation along a curved membrane in a magnetic field would result in a greater rate of change of the local quadrupolar (^{2}H) or shielding (^{31}P) field with consequent increase in the nuclear spin relaxation rate [17]. Increased equilibrium curvature would also correlate with a decrease in the activation energy needed to reach highly curved fusion intermediates and a consequent increase in the fusion rate [1,13].

The HFP-induced curvature interpretation of the NMR results is consistent with other experimental data. X-ray measurements of DOPC membranes with and without bound HFP were interpreted in terms of HFP-induced reduction of the bending modulus of the membranes which would result in more highly curved membranes [48]. Differential scanning calorimetry has shown that the 16-residue N-terminal portion of HFP lowers the transition temperature of PE membranes from lamellar to inverted hexagonal phase, and this result was interpreted in terms of HFP-induction of negative membrane curvature [9]. As observed in earlier studies as well as the present work, ^{31}P NMR spectra of HFP bound to PE-rich membranes are consistent with isotropic membrane phases [8]. Such phases have been interpreted as arising from highly curved lipid structures such as small vesicles or a cubic phase [24,49]. Thus, the curvature interpretation of our results is consistent with interpretation of other experimental data and with a reasonable general mechanism for HFP-induced catalysis of membrane fusion. It is noted, however, that the induction of curvature by the HFP is not a unique or definitive interpretation of our data.

Acknowledgment

We acknowledge support from NIH AI47153.

References

[1] J.M. White, S.E. Delos, M. Brecher, K. Schornberg, Structures and mechanisms of viral membrane fusion proteins: multiple variations on a common theme, Crit. Rev. Biochem. Mol. Biol. 43 (2008) 189–219.
[2] S.R. Durell, I. Martin, J.M. Ruysschaert, Y. Shai, R. Blumenthal, What studies of fusion peptides tell us about viral envelope glycoprotein-mediated membrane fusion, Mol. Membr. Biol. 14 (1997) 97–112.
[3] W. Qiang, M.L. Bodner, D.P. Weliky, Solid-state NMR spectroscopy of human immunodeficiency virus fusion peptides associated with host-cell-like membranes: 2D correlation spectra and distance measurements support a fully extended conformation and models for specific antiparallel strand registries, J. Am. Chem. Soc. 130 (2008) 5459–5471.
[4] W. Qiang, J. Yang, D.P. Weliky, Solid-state nuclear magnetic resonance measurements of HIV fusion peptide to lipid distances reveal the intimate contact of beta strand peptide with membranes and the proximity of the Ala-14-Gly-16 region with lipid headgroups, Biochemistry 46 (2007) 4997–5008.
[5] W. Qiang, D.P. Weliky, HIV fusion peptide and its cross-linked oligomers: efficient syntheses, significance of the trimer in fusion activity, correlation of β strand conformation with membrane cholesterol, and proximity to lipid headgroups, Biochemistry 48 (2009) 289–301.
[6] R.F. Epand, I. Martin, J.-M. Ruysschaert, R.M. Epand, Membrane orientation of the SIV fusion peptide determines its effect on bilayer stability and ability to promote membrane fusion, Biochem. Biophys. Res. Comm. 205 (1994) 1938–1943.
[7] A. Schanck, J. Peuvot, R. Brasseur, Influence of the mode of insertion of SIV peptides into membranes on the structure of model membrane as studied by ^{31}P NMR, Biochem. Biophys. Res. Commun. 250 (1998) 12–14.
[8] F.B. Pereira, J.M. Valpuesta, G. Basanez, F.M. Goni, J.L. Nieva, Interbilayer lipid mixing induced by the human immunodeficiency virus type-1 fusion peptide on large unilamellar vesicles: the nature of the nonlamellar intermediates, Chem. Phys. Lipids 103 (1999) 11–20.
[9] S.G. Peisajovich, R.F. Epand, M. Pritsker, Y. Shai, R.M. Epand, The polar region consecutive to the HIV fusion peptide participates in membrane fusion, Biochemistry 39 (2000) 1826–1833.
[10] R.M. Epand, Lipid polymorphism and protein–lipid interactions, Biochim. Biophys. Acta 1376 (1998) 353–368.
[11] D.P. Siegel, The energetics of intermediates in membrane fusion: comparison of stalk and inverted micellar intermediate mechanisms, Biophys. J. 65 (1993) 2124–2140.

[12] D.P. Siegel, R.M. Epand, The mechanism of lamellar-to-inverted hexagonal phase transitions in phosphatidylethanolamine: implications for membrane fusion mechanisms, Biophys. J. 73 (1997) 3089–3111.
[13] R.M. Epand, Fusion peptides and the mechanism of viral fusion, Biochim. Biophys. Acta 1614 (2003) 116–121.
[14] M. Bloom, E. Evans, O.G. Mouritsen, Physical properties of the fluid lipid-bilayer component of cell membranes: a perspective, Quart. Rev. Biophys. 24 (1991) 293–397.
[15] J. Seelig, Deuterium magnetic resonance: theory and application to lipid membranes, Quart. Rev. Biophys. 10 (1977) 353–418.
[16] J. Seelig, A. Seelig, Lipid conformation in model membranes, Quart. Rev. Biophys. 13 (1980) 19–64.
[17] M. Bloom, E. Sternin, Transverse nuclear spin relaxation in phospholipid bilayer membranes, Biochemistry 26 (1987) 2101–2105.
[18] C.D. Chang, M. Waki, M. Ahmad, J. Meienhofer, E.O. Lundell, J.D. Haug, Preparation and properties of N-α-9-fluorenylmethyloxycarbonylamino acids bearing tert-butyl side chain protection, Int. J. Pept. Protein Res. 15 (1980) 59–66.
[19] L. Lapatsanis, G. Milias, K. Froussios, M. Kolovos, Synthesis of N-2,2,2-(trichloroethoxycarbonyl)-L-amino acids and N-(9-fluorenylmethoxycarbonyl)-L-amino acids involving succinimidoxy anion as a leaving group in amino-acid protection, Synthesis 8 (1983) 671–673.
[20] E.O. Freed, E.L. Delwart, G.L. Buchschacher Jr., A.T. Panganiban, A mutation in the human immunodeficiency virus type 1 transmembrane glycoprotein gp41 dominantly interferes with fusion and infectivity, Proc. Natl. Acad. Sci. U. S. A. 89 (1992) 70–74.
[21] F.B. Pereira, F.M. Goni, J.L. Nieva, Liposome destabilization induced by the HIV-1 fusion peptide effect of a single amino acid substitution, FEBS Lett. 362 (1995) 243–246.
[22] C.M. Wasniewski, P.D. Parkanzky, M.L. Bodner, D.P. Weliky, Solid-state nuclear magnetic resonance studies of HIV and influenza fusion peptide orientations in membrane bilayers using stacked glass plate samples, Chem. Phys. Lipids 132 (2004) 89–100.
[23] C.E. Dempsey, The actions of melittin on membranes, Biochim. Biophys. Acta 1031 (1990) 143–161.
[24] A. Naito, T. Nagao, K. Norisada, T. Mizuno, S. Tuzi, H. Saito, Conformation and dynamics of melittin bound to magnetically oriented lipid bilayers by solid-state ^{31}P and ^{13}C NMR spectroscopy, Biophys. J. 78 (2000) 2405–2417.
[25] R.C. Aloia, H. Tian, F.C. Jensen, Lipid composition and fluidity of the human immunodeficiency virus envelope and host cell plasma membranes, Proc. Natl. Acad. Sci. U. S. A. 90 (1993) 5181–5185.
[26] B. Brugger, B. Glass, P. Haberkant, I. Leibrecht, F.T. Wieland, H.G. Krasslich, The HIV lipidome: a raft with an unusual composition, Proc. Natl. Acad. Sci. U.S.A. 103 (2006) 2641–2646.
[27] D.K. Struck, D. Hoekstra, R.E. Pagano, Use of resonance energy transfer to monitor membrane fusion, Biochemistry 20 (1981) 4093–4099.
[28] J. Yang, C.M. Gabrys, D.P. Weliky, Solid-state nuclear magnetic resonance evidence for an extended beta strand conformation of the membrane-bound HIV-1 fusion peptide, Biochemistry 40 (2001) 8126–8137.
[29] F.B. Pereira, F.M. Goni, A. Muga, J.L. Nieva, Permeabilization and fusion of uncharged lipid vesicles induced by the HIV-1 fusion peptide adopting an extended conformation: dose and sequence effects, Biophys. J. 73 (1997) 1977–1986.
[30] T. Gullion, J. Schaefer, Rotational-echo double-resonance NMR, J. Magn. Reson. 81 (1989) 196–200.
[31] A.E. Bennett, C.M. Rienstra, M. Auger, K.V. Lakshmi, R.G. Griffin, Heteronuclear decoupling in rotating solids, J. Chem. Phys. 103 (1995) 6951–6958.
[32] T. Gullion, D.B. Baker, M.S. Conradi, New, compensated Carr-Purcell sequences, J. Magn. Reson. 89 (1990) 479–484.
[33] T. Gullion, J. Schaefer, Elimination of resonance offset effects in rotational-echo, double-resonance NMR, J. Magn. Reson. 92 (1991) 439–442.
[34] C.R. Morcombe, K.W. Zilm, Chemical shift referencing in MAS solid state NMR, J. Magn. Reson. 162 (2003) 479–486.
[35] D.I. Hoult, R.E. Richards, Critical factors in the design of sensitive high resolution nuclear magnetic resonance spectrometers, Proc. R. Soc. Lond., Ser. A 344 (1975) 311–340.
[36] R. Yang, M. Prorok, F.J. Castellino, D.P. Weliky, A trimeric HIV-1 fusion peptide construct which does not self-associate in aqueous solution and which has 15-fold higher membrane fusion rate, J. Am. Chem. Soc. 126 (2004) 14722–14723.
[37] J. Yang, P.D. Parkanzky, M.L. Bodner, C.G. Duskin, D.P. Weliky, Application of REDOR subtraction for filtered MAS observation of labeled backbone carbons of membrane-bound fusion peptides, J. Magn. Reson. 159 (2002) 101–110.
[38] J. Yang, M. Prorok, F.J. Castellino, D.P. Weliky, Oligomeric beta structure of the membrane-bound HIV-1 fusion peptide formed from soluble monomers, Biophys. J. 87 (2004) 1951–1963.
[39] H.Y. Zhang, S. Neal, D.S. Wishart, RefDB: a database of uniformly referenced protein chemical shifts, J. Biomol. NMR 25 (2003) 173–195.
[40] C.P.S. Tilcock, P.R. Cullis, S. Gruner, On the validity of ^{31}P determinations of phospholipid polymorphic phase behaviour, Chem. Phys. Lipids 40 (1986) 47–56.
[41] L. Rilfors, P.-O. Eriksson, G. Arvidson, G. Lindblom, Relationship between three-dimensional arrays of "lipidic particles" and bicontinuous cubic lipid phases, Biochemistry 25 (1986) 7702–7711.
[42] E. Shyamsunder, S.M. Gruner, M.W. Tate, D.C. Turner, P.T.C. So, C.P.S. Tilcock, Observation of inverted cubic phase in hydrated dioleoylphosphatidylethanolamine membranes, Biochemistry 27 (1988) 2332–2336.
[43] P.R. Cullis, B. DeKruijff, ^{31}P NMR studies of unsonicated aqueous dispersions of neutral and acidic phospholipids — effects of phase transitions, p^{2}H and divalent cations on the motion in the phosphate region of the polar headgroup, Biochim. Biophys. Acta 436 (1976) 523–540.
[44] K. Sackett, M.J. Nethercott, Y. Shai, D.P. Weliky, Hairpin folding of HIV gp41 abrogates lipid mixing function at physiologic pH and inhibits lipid mixing by exposed gp41 constructs, Biochemistry 48 (2009) 2714–2722.
[45] C. Curtain, F. Separovic, K. Nielsen, D. Craik, Y. Zhong, A. Kirkpatrick, The interactions of the N-terminal fusogenic peptide of HIV-1 gp41 with neutral phospholipids, Eur. Biophys. J. 28 (1999) 427–436.
[46] J. Yang, P.D. Parkanzky, B.A. Khunte, C.G. Canlas, R. Yang, C.M. Gabrys, D.P. Weliky, Solid state NMR measurements of conformation and conformational distributions in the membrane-bound HIV-1 fusion peptide, J. Mol. Graph. Model. 19 (2001) 129–135.
[47] P. Agrawal, S. Kiihne, J. Hollander, F. Hulsbergen, M. Hofmann, D. Langosch, H. de Groot, Solid state NMR investigation of the interaction between biomimetic lipid bilayers and de novo designed fusogenic peptides, Chembiochem 8 (2007) 493–496.
[48] S. Tristram-Nagle, J.F. Nagle, HIV-1 fusion peptide decreases bending energy and promotes curved fusion intermediates, Biophys. J. 93 (2007) 2048–2055.
[49] A. Colotto, R.M. Epand, Structural study of the relationship between the rate of membrane fusion and the ability of the fusion peptide of influenza virus to perturb bilayers, Biochemistry 36 (1997) 7644–7651.